

# Shuffle SwishNet-181: COVID-19 diagnostic framework using ECG images

Tanees Riaz<sup>1</sup> · Ali Javed<sup>1</sup> · Majed Alhazmi<sup>2</sup> · Ali Tahir<sup>2</sup> · Rehan Ashraf<sup>3</sup>

Received: 10 October 2022 / Revised: 25 May 2023 / Accepted: 17 October 2023 / Published online: 2 November 2023

© The Author(s), under exclusive licence to Springer Science+Business Media, LLC, part of Springer Nature 2023

#### Abstract

Early and precise detection of COVID-19 holds significant benefits, particularly in facilitating the prompt isolation of infected individuals and helping to control the spread of this disease as vaccinated persons also got infected from COVID-19. The research community has explored various COVID-19 diagnostic tools operated on different imaging modalities like X-rays and CT scans apart from conventional PCR testing which often takes several hours to get the results. Existing studies on ECG-based COVID-19 diagnostics are limited even though this modality is quickly available as compared to CT scans and X-rays. Moreover, our preliminary analysis suggests that ECG images can also be used to study the correlation of COVID-19 with cardio diseases, which is not possible in the case of X-rays and CT scans. Moreover, current ECG-based COVID-19 diagnostics approaches often report an issue of low detection accuracy and focus more on binary classification. To overcome these challenges, we developed an effective COVID-19 diagnostic tool by proposing a novel Shuffle SwishNet-181 deep learning-based model. During the pre-processing, the background is subtracted from the signals and combined these signals in a hexaxial way. Shuffle SwishNet-181 extracts the distinctive deep features and accurately classifies the ECG images into COVID-19, normal, myocardial infarction (MI), abnormal heartbeat patients (HB), and patients who have a history of myocardial infarction (PMI). Moreover, the Score-cam technique is employed to visualize the working of the proposed model by showing the top priority features extracted by the Shuffle SwishNet-181 model. The rigorous experimentation is performed on a publicly available ECG imaging dataset to demonstrate the effectiveness of the COVID-19 diagnostic framework. The proposed model achieved an accuracy of 99% in the case of COVID-19 vs. Normal, 99.4% in the case of COVID-19 vs. MI, 98.8% in the case of COVID-19 vs. HB, and 98.7% in the case of COVID-19 vs. PMI. For multiclass classification, the proposed model achieved 91.6% accuracy. Experimental results show the reliability of the method for binary and multiclass classification of COVID-19. Explainability analysis proved that the proposed model precisely focuses on salient features for classification.

**Keywords** COVID-19 detection · Cardiovascular patients · ECG · Shuffle SwishNet-181

Extended author information available on the last page of the article



Rehan Ashraf rehan@ntu.edu.pk

## 1 Introduction

The world is facing the deadliest pandemic "COVID-19" and its disasters are increasing day by day. COVID-19 started in the city of Wuhan; China has now spread to all countries. The virus is not only spreading at a higher rate but is also changing its RNA and creating its mutants. Till now 256,966,237 cases have been reported along with 5,151,643 deaths all around the world [22]. COVID-19 symptoms vary from no symptoms to mild and severe symptoms. Studies have shown that COVID-19 affects different organs therefore it has a large variety of symptoms. In mild cases, fever, cough, sore throat, tiredness, high temperature, sneezing, diarrhea, headache, loss or disturbance in the sense of smell and/or taste are the most common symptoms that have been seen in infected persons [23]. Severe symptoms include shortness of breath which in certain cases can cause death. Research has shown that COVID-19 produces double pneumonia in the lungs [29]. COVID-19 not only affects the lungs but also disturbs the working of the heart, kidneys, and brain. Chowdhry et al. studied the harmful effect of COVID-19 on body organs. The study concluded that dysregulation and thrombotic microangiopathy, and "cytokine storm" syndrome are the factors that are harmful to kidneys during COVID-19. Moreover, the COVID-19 virus can attach to ACE-2 receptors through which the virus can invade in brain, liver, kidney, and heart causing a multi-organ failure [7]. COVID-19 has not only asymptomatic in nature but also transmit at a rapid rate that urges for fast and accurate detection of an infected person.

Different testing approaches have been introduced till now for the detection of COVID-19. Clinicians are using different techniques, which include Nucleic Acid testing, Protein testing, and computed tomography for the diagnosis of COVID-19. Among several testing procedures, nucleic acid testing using real-time reverse transcriptase-polymerase chain reaction (rRT-PCR) for amplification of nucleic acid is the most accustomed testing technique. rRT-PCR is a standard technique that uses samples taken from the nasopharynx (uppermost part of the nose and throat) and detects the presence of the pathogen in the sample. The patient gets the results of the test from 12 h to 5 days at a high cost. Protein testing uses the antigens and antibodies that are generated by the body in response to the COVID-19 attack on the body. There is no critical amplification process in it therefore it is rapid, easy, and does not need skilled staff. Missing amplification process produced on a very less amount of sample which leads to inaccurate results [15]. However, each technique has its drawbacks and including RT-PCR, there is no such technique till now that produces the most accurate results at all times. Nucleic acid testing may show COVID-19-positive patients as negative which is the main drawback of this technique. Moreover, special kits and a laboratory setup are required for testing COVID-19 through nucleic acid testing and protein testing. This situation urges the development of detection systems that use already existing technologies and do not need any specialized laboratory setup.

AI-based methods are also developed which use existing technology for the identification of COVID-19-infected persons. When AI-based models are utilized in the medical profession, there is a risk that the model will make decisions based on irrelevant features. However, advances in artificial intelligence also help in interpreting the working of CNN. Explainable AI gives solutions to these problems and clarifies the working of CNN models. Manga et al. [4] worked on the four categories of X-ray images normal, bacterial pneumonia, viral pneumonia, and COVID-19 pneumonia. The study developed a 121-layer deep DenseNet CNN model to classify X-ray images into four categories. Garzon et al. [8] applied current deep learning models (VGG19 and U-Net) to identify images as positive or negative for COVID-19. The study utilized segments of lung X-rays that removed

the surrounding's irrelevant information for the classification that might produce biased results, a transfer learning-based model was used for classification. Other infections also cause pneumonia in the lungs in such conditions making the identification process complex. Moreover, much research is performed on the detection of COVID-19 using CT and chest X-rays, but these researches ignore the effect of COVID-19 on major body organs including the heart.

Researchers have observed that COVID-19 has a harmful effect on the heart. Ibrahim et al. compared the ECG of 105 COVID-19 patients having a mean age of 11 with a healthy control group. The COVID-19 symptoms in children were of mild or asymptomatic category in comparison with adults. In the study, among 105 children, 51.4% of cases showed no symptoms and 48.5% of cases showed mild symptoms. The research proved that there was a major difference in heart rate between the COVID-19 patient's ECG and the control group's ECG. The study concluded that the risk of ventricular arrhythmia may increase and there was a modification in repolarization characteristics in such asymptomatic patients [18]. Kaliyaperumal et al. [9] studied the ECG of COVID-19 patients when they were admitted in the hospital. The study found that 81% of ECGs were abnormal, where 2.9% had rhythm abnormalities, 36.5% of patients showed rate abnormalities, and 2.9% of patients dealt with prolonged PR intervals. A significant change in ST and T segments was observed in 42.9% of patients. This study proved that ECG can be a highly beneficial tool for the diagnosis of COVID-19. Even though COVID-19 influences heart working not only in critical cases but also in asymptomatic cases, few experiments are done for the detection of COVID-19 using ECG. Barman found that 7 to 28% of patients developed acute heart abnormalities during COVID-19. Based on severity, patients were divided into severe and none-severe groups. The study concluded that abnormalities in ECG increase with a surge in the severity of COVID-19 infection [16].

Characteristics of patients who are detected with COVID-19 have clearly shown that the heart is infected when the virus attacks the body [18]. Therefore, ECG can be a beneficial tool for the diagnosis of COVID-19-positive patients. Existing methods that use ECG for the identification of COVID-19 have low accuracy problems. Currently, clinicians are using five different types of molecular and antigen testing techniques for the recognition of COVID-19. These testing techniques need expert personnel with a proper laboratory setup and specialized primers which are difficult to design. Moreover, rRT-PCR is the most sensitive technique used for detection, but it takes several hours for execution. This research aims to provide an automated method to detect COVID-19 more precisely and quickly. This research suggested an approach that implements deep learning-based models to detect COVID-19 based on abnormalities developed in an infected patient's ECG. The proposed model classifies ECG images of COVID-19 patients and ECGs of non-COVID-19 persons which include Normal, Myocardial Infarction, Abnormal Heartbeat, and Patients with history of any Myocardial Infarction. The model effectively classifies COVID-19-positive patients in a multiclass scenario. The main contributions of our work are:

- Development of an effective end-to-end deep learning model for reliable detection of COVID-19 from the ECG images.
- Development of effective deep features capable of extracting distinctive traits from the ECG images of normal people and COVID-19 patients.
- Explainability analysis to visualize the discriminatory features selected by our model to achieve reliable classification.
- Performance improvement over the existing contemporary ECG-based COVID-19 detection methods.

Section 2 of the paper presents an overview of the existing research conducted on the detection of COVID-19 through analysis of electrocardiogram (ECG) images. In Section 3, we present a comprehensive description of the proposed methodology. Moving forward to Section 4, we provide an extensive analysis of the experiments conducted to assess the effectiveness of the proposed methodology, accompanied by a thorough discussion of the obtained results. Finally, Section 5 concludes our study, summarizing the key findings and suggesting avenues for further research in this domain.

#### 2 Related work

This section presents a critical investigation of existing state-of-the-art COVID-19 detection and analysis methods. Section 2.2 discusses the adverse effects of COVID-19 on the heart as well as the ECG characteristics of COVID-19 patients.

## 2.1 Automated testing using CT scans and x-rays

Radiological images serve as an advantageous tool for the identification of COVID-19. COVID-19 affects the human respiratory system. Existing methods have utilized different deep learning frameworks including transfer learning to develop COVID-19 detection methods CT scans and X-rays. Hussain [13] presented a 22-layer CNN model "CoroDet" which utilized X-ray images and CT-scan images as input to develop 2-class and multiclass classification for COVID-19. This model achieved 99.1% accuracy for 2-class, 94.2% during 3-class, and 91.2% during 4-class classification. These methods solve the problem of low sensitivity in molecular and protein testing. Wong et al. [17] studied features of chest X-rays of COVID-19-infected persons. The distribution of these features was found at 41% in the peripheral area and 50% in the lower area of the lungs. Wang et al. [25] suggested a CNN prediction model for the identification of COVID-19 by employing explainable AI methods. The model used three categories of lung X-ray images that are non-COVID-19, normal, and COVID-19-affected images. The model achieved 92.4% accuracy to predict COVID-19 cases. This prediction model helps clinicians to diagnose critical cases. However, such models are developed on a limited data set and most studies used COVID-19 negative images from a different dataset which leads to good results [19].

#### 2.2 ECG an important tool for COVID-19 detection

Heartbeat produces electrical signals that are recorded in the form of an ECG providing the current condition of the heart. ECG can detect ischemia, atrial fibrillation, left ventricular hypertrophy, and even an early diagnosis of cardiovascular diseases [21]. 12-Lead ECG is considered the most used standard lead. Each lead provides a different angle for an electrical potential drop between two points in space. The frontal plane contains six leads I, II, III, avF, avR, and avL, known as limb leads which detect the vector in the frontal plane while the horizontal plane contains V1, V2, V3, V4, V5, V6, known as chest leads which detects the vector in the horizontal plane. Leads I-III are the original leads obtained from one exploring electrode and two reference electrodes and the other 9 leads are obtained from one exploring electrode and a combination of three or two reference electrodes [12]. The hexaxial reference system is used to represent six limbs lead in the frontal plane. This reference system contributes to giving a more explainable sequence of leads for reading

the ECG. This system uses an order of lead as avL, I, the inverse of avR, II, avF, III, and then V1 to V6. Inverted avR assists to find inferior myocardial infarctions, moreover, it also fills the space between leads II and III moving toward the right or left in the reference system [11]. Research has shown that the ECG of COVID-19 patients has particular features that make them identifiable. Angeli et al. [14] defined the ECG features of COVID-19 patients having pneumonia. The team examined 12-Lead-ECG of 50 COVID-19 patients at the time of admission, on worsening clinical conditions, and before discharge. The study showed that 26% of patients developed new ECG abnormalities. Angeli et al. concluded that COVID-19 patients get ECG abnormalities at later stages and these included a broad range of cardiovascular abnormalities. Li et al. [26] used 18-Lead ECG and laboratory tests for observing the effect of COVID-19 on its victims. ECG was measured at the time of admission of patients and when the patient's condition becomes adverse the study showed the comparison of ECG conditions between non-ICU patients and ICU patients. Li et al. found that patients with cardiovascular problems also got ECG abnormalities due to COVID-19. Kaliyaperumal et al. [6] studied the ECG of COVID-19 patients before and during COVID-19. During the study, patients were divided into two groups, and their PR: HR slopes were analyzed. Pavri et al. found that PR prolongation with an increase in heart rate in COVID-19 patients was even a cause of death in some cases. The study has a limitation because PR-interval measurement may be susceptible to error.

## 2.3 ECG image classification

The majority of the imaging modality-based works presented for COVID-19 detection have used either CT or X-ray images. Acharya et al. [1] proposed a feasibility study of using deep convolutional neural networks (CNNs) for COVID-19 detection using ECG signals. The study evaluated several pre-trained CNN models, including AlexNet, VGG16, and ResNet50, for COVID-19 detection. The results showed that these models achieved high accuracy for COVID-19 detection, with ResNet50 achieving the highest accuracy of 96.67%. There have been several deep-learning models proposed for COVID-19 detection using ECG images. According to our knowledge, there exist a few works that have used ECG images for COVID-19 detection due to the limited availability of ECG-based COVID-19 datasets. As per our investigation, there is only one publicly available dataset called the ECG Images dataset of Cardiac Patients [3] that contains COVID-19 ECG images till now. Studies done on COVID-19 diagnosis through ECG used this same dataset for evaluation.

In a recent study, Dey et al. [10] suggested an ECG-based pipeline for COVID-19 diagnosis called ECG-BiCoNet that utilized Bi-Layers of deep features integration. These deep features were then integrated and fed into a classifier for COVID-19 diagnosis. The pipeline accomplished an accuracy of 99.5% for COVID-19 diagnosis. One of the limitations of the "ECG-BiCoNet" pipeline is the large amount of data required for training due to the use of two Bi-Layer modules for feature extraction. The high number of parameters in these modules results in a risk of overfitting, making a large dataset necessary for accurate COVID-19 detection. Attallah [5] introduced the ECG-BiCoNet model which extracts bilevel characteristics from two separate layers of five different deep learning models. Bilevel features were combined to feed into an ensemble classification model which used three ML classifiers. Experiments obtained an accuracy of 98.8% on binary classification and 91.73% on multi-class. The study does not provide details of classification with other cardiovascular classes. Mehmet et al. [20] employed ECG-based images for classifying

COVID-19 patients. The study used the Gray-Level Co-Occurrence Matrix (GLCM) for extracting features from images and implemented the hexaxial method for mapping of converted features into 2-D images. Studies performed classification using a deep learning model which achieved 96.02% accuracy for a normal vs. COVID-19 case while 93% for COVID-19 vs. no findings. The authors of the study converted ECG images into numerical features and again converted these features into image form, this conversion process may introduce errors in the results. Moreover, the study did not provide the effectiveness of the model in the presence of all cardiovascular diseases. Tawsifur et al. [24] compared pre-trained deep learning models: ResNet18, InceptionV3, ResNet50, MobileNetv2, ResNet101, and DenseNet201 on ECG images. InceptionV3 performed best among all CNN in a five-class problem by achieving 97.83% accuracy. However, in binary and threeclass problems, DenseNet-201 attained the highest accuracy of 99.1% and 97.36%, respectively. Despite good results, the study did not perform preprocessing on images which may lead to performance degradation and used fewer data for testing which may introduce the biasing problem. Anwar et al. [27] studied the impact of augmentation while the classification of ECG-based images. The study concluded that to some extent, augmentation assists to increase the accuracy, but multiple data augmentation techniques can ultimately reduce the accuracy. This study was able to obtain an accuracy of 81% without augmentation. This study did not achieve promising results. Ahmed et al. introduced a deep-learning model to detect COVID-19 vs Normal ECG images. The study achieved 98.81% average accuracy. During experiments, the different CNN models utilized direct ECG images for classification. The study focused more on binary classification. Moreover, the authors of the study utilized imbalanced data for experiments [2].

## 3 Proposed methodology

This section presents a detailed explanation of the proposed ECG-based COVID-19 detection method. Preprocessing is performed on ECG images since the images contain noise. After Preprocessing the images are resized according to the developed CNN model "Shuffle SwishNet-181" and these images are fed into the model. The first layers extract deep features from the preprocessed ECG images and pass the extracted deep features to classification layers. The Shuffle SwishNet-181 is designed to extract deep features from the ECG images using a series of convolutional and pooling layers. The convolutional layers implement filters to the preprocessed images to perceive features such as edges and patterns, while the pooling layers reduce the dimensions in the spatial aspect to capture the most salient information in the images. The convolutional layers output is transferred to fully connected layers, which deploys a final classification of the ECG image as COVID-19 positive or negative. The fully connected layers aggregate the extracted features and use them to make a prediction based on the learned patterns in the data. The detailed methodology is provided in subsequent subsections.

## 3.1 Preprocessing

The available dataset contains unprocessed images which require preprocessing techniques to generate classifiable images. Initially, few images were the ECG reports of the patient which includes irrelevant information. The irrelevant information was removed to separate the ECG part only. Each image contains the data of 12 leads and leads II or III signals; the data of each

lead is separated by dividing the entire image into different lead images. Each lead starting and ending point is manually set to take out the required part of the image. The next step is the removal of background and labels from all lead images. For this purpose, the segmentation and closing operation is employed. The results of the background removal process are white lines that represent the signals while having a black background. To set images in a hexaxial way, the mirror images of six leads (I, II, III, avF, avR, and avL) were generated to show the inverse signal of these leads. To concatenate all lead images including mirror images in 3 rows and six columns to generate the final image. A sequence of the combination of leads in every image is shown in Table 1. In order to meet the requirement of the proposed deep learning model, the input images were resized to  $224 \times 224 \times 3$ . During the background removal process, all images were converted into binary format, therefore, all images were first converted into a 3-channel image and then resized to  $224 \times 244$ .

The objective of this study is to diagnose and detect COVID-19-positive patients through ECG trace images. The proposed model used an improved ShuffleNet architecture named Shuffle SwishNet-181 for extracting deep features and classification of ECG images. The proposed model contains three steps: pre-processing of ECG images, feature extraction of preprocessed ECG images, and classification of deep features. Image preprocessing is necessary as the available dataset is in raw format. During preprocessing, 6 leads (I, II, III, avF, avR, avL) are inversed. There are two main reasons for inversing these leads; the hexaxial system is a reference system to present ECG in a 2D image format. This reference system places the Lead I at 0° position and all other leads are placed according to Lead I. Inverse Lead avR is used in this system which helps to detect inferior myocardial infarction. Moreover, the inversion of the limb leads also provides another angle to show heart electrical activity which assists in identifying COVID-19 patients. The images of limb leads, the inverse of limb leads, and chest leads are combined to form one image. The generated images are then fed to the novel Shuffle SwishNet-181 DL model for feature extraction. Shuffle SwishNet-181 extracts the deep features from the input images and later classifies them into COVID-19, Myocardial Infarction (MI), Abnormal Heartbeat (HB), Normal, or Previous Myocardial Infarction (PMI) classes. Figure 1 shows the working of the proposed model.

#### 3.2 Pre-trained deep learning model

Deep learning approaches are widely used in medical imaging for the detection and monitoring of patients. Several pre-trained deep learning models are available for example resnet-50, resnet-18, AlexNet, and ShuffleNet. These networks are trained on the ImageNet database containing 1000 classes. ShuffleNet is a deep learning architecture designed for efficient and accurate image classification, which achieves state-of-the-art results with low computational complexity. It was proposed by Zhang et al. [28] as a modification to the traditional convolutional neural network (CNN) architecture, utilizing group convolutions and channel shuffling to reduce the number of parameters and computation required, thus resulting in faster training and inference times. Group convolutions enable the network to learn more efficient and effective feature representations by reducing the computational complexity and the number of

**Table 1** Leads arrangement in the final image

I	avL	III(-)	avF(-)	II(-)	avR(-)
I(-)	avL(-)	III	avF	II	avR(-)
V1	V2	V3	V4	V5	V6

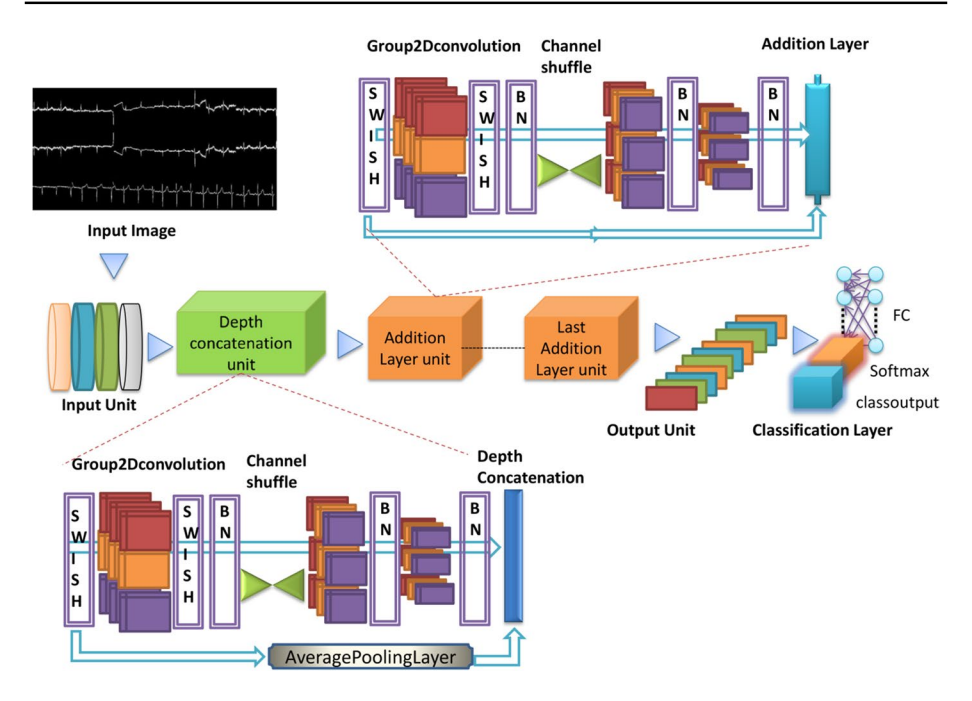


Fig. 1 Proposed model

parameters. Channel shuffling allows for inter-group communication and enhances the diversity of feature maps, making the network more robust and accurate. Compared to traditional CNNs, ShuffleNet demonstrates superior accuracy and computational efficiency, making it a popular choice for resource-constrained scenarios.

ShuffleNet is comparable to AlexNet in terms of performance but ShuffleNet has 13 times lower computational cost than AlexNet. ShuffleNet performs image classification effectively and efficiently therefore, we selected the ShuffleNet architecture for enhancement. ShuffleNet consists of channel shuffle on group convolution and Shuffle unit. ShuffleNet consists of 172 layers in which global average pooling passes deep features to the last three layers (fully connected, softmax, and classification) to perform the classification.

#### 3.2.1 Shuffle SwishNet-181

The proposed Shuffle SwishNet-181 model comprises 181 layers that include nine additional layers of group2dconvolution, batch Normalization, and Swish layer as compared to 172 layers of the pre-trained ShuffleNet model. These expanded layers do not follow the basic architecture of shuffle unit blocks rather these layers are present in a repeated sequence. This enhanced the performance of the pre-trained ShuffleNet on the available dataset. Shuffle SwishNet-181 layers are divided into different units; the last nine layers form the output unit, and the last layer of this unit passes the output features to the classification layers. Moreover, ShuffleNet utilizes the ReLU activation function in all of its layers. ReLU units can suffer from the "dying ReLU" problem where the units can become inactive and stop responding to any input signal during training. This can lead to reduced learning capacity and slower convergence rates, especially in deep networks.



The Swish activation function is a recently proposed alternative to the ReLU function, which has demonstrated improved performance in several deep learning models. Swish is bounded, which can help prevent the numerical instability and diverging gradients that can occur with ReLU. Therefore, instead of ReLU activation function that is used in traditional ShuffleNet, Shuffle SwishNet-181 employs the swish activation function which enhances the classifying capability of architecture.

Figure 2 shows the input and output units used in the creation of Shuffle Swish-Net-181. Group2dconvolution is a conventional convolution that is separated into groups with different depths. Group convolution enhances the efficiency of a model because the number of parameters decreased as the number of filter groups increases. Moreover, grouped convolution helps to develop a better model. Our proposed Shuffle SwishNet-181 model consists of 181 layers of which the last three layers are involved in the classification task. The input layer takes a  $224 \times 224 \times 3$  sized image and passes it to the convolution layer followed by batch Normalization, swish layer, and Maxpooling layer. After the MaxPooling layer, a set of layers starts which contains the swish layer, 2d group convolution layer, batch Normalization, and swish layer followed by a shuffle unit which shuffles the next four layers. The inputs from the swish and batch normalization layers are combined using an additional layer. Following the last additional layer, there are 9 layers in a repeated sequence of 2D Group convolution, batch normalization, and swish. The last swish layer passes all the extracted deep features to the Global average pooling layer and finally to the last three layers namely Fc, Softmax, and class output layers for the classification.

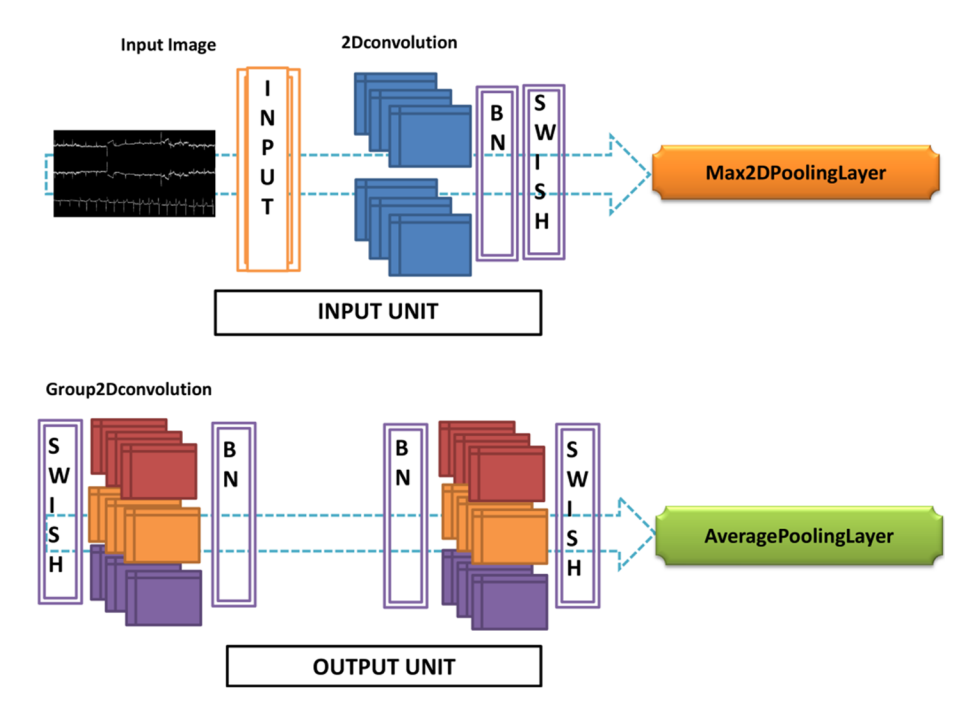


Fig. 2 Input and output units

## 3.2.2 Additional layer units and depth concatenation unit

Shuffle SwishNet-181 uses group convolution in all units except the input unit. A drawback of group convolution is that it sometimes blocks feature communication among different groups. The shuffle channel solves this issue of group convolution among different convolution units. Channel shuffle merges and reorganizes all information from different convolution units to share the features with other filters as well. This allows the flow of features among all filters and resists the blocking of information. Hence, allowing better performance of the proposed model for the classification of ECG images. An additional layer is then used to take input from different layers and add them element-wise. In-depth concatenation unit, the average pooling layer is used to down-sample the feature map to the average value of that patch. The depth concatenation unit takes input from the average pooling layer and batch normalization layer and combines them in a third dimension which is the dimension of the input channel. Figure 1 shows the layers involved in the Shuffle unit and depth concatenation unit.

#### 3.3 Swish activation

The activation function can influence the training of CNN models significantly. The basic architecture of ShuffleNet uses the RELU activation function. RELU activation function is commonly used in deep learning models but it has 0 derivative problems for half of its input values which becomes a reason for 40% of dead neurons in the neural network. Swish has outperformed RELU and improved training for various deep learning networks. It also works better for complex and challenging image classification tasks. Swish activation function uses sigmoid function as shown in Eqs. (1) and (2). In our proposed method, the swish activation function is used instead of RELU, which assists to improve the classification of ECG images.

$$Swish = x \cdot sigmoid(x) \tag{1}$$

where

$$sigmoid(x) = \frac{1}{1 + e^{-x}} \tag{2}$$

## 4 Results and discussion

This section contains a discussion of the results of experiments conducted to investigate the performance of our method. Details of the dataset on which we evaluated our method are also discussed. Information on evaluation metrics is also provided in this section.

## 4.1 Dataset

We have used a publicly available ECG dataset [3] for the evaluation of our method. According to our knowledge, this is the only publicly accessible ECG image dataset of COVID-19 patients now. Haider et al. collected this data from various medical institutes



in Pakistan using the 'EDAN SERIES-3 device. The first version of this dataset consists of 1937 images of 12-Lead ECG signals which are manually classified into 5 categories by medical professionals. The first version contains 250 images of COVID-19, 77 images of myocardial infarction (MI), 548 images of abnormal heartbeat, 859 normal images, and 203 images having a previous myocardial infarction (PMI). However, the second version does not include the category of COVID-19 but the number of images is increased in other categories. All of these images are in raw format and a 500 HZ sampling rate is used for collecting this data. The COVID-19 category includes the data of those who tested positive and are in isolation. The myocardial infarction category includes the data of those who have severe heart conditions and are in ICU. The abnormal heartbeat contains the data of those who have recovered from COVID-19 or MI and have heartbeat abnormality issues. Those who have any history of myocardial infarction or heart attack fall in the previous myocardial infarction category while those who do not have any kind of ECG abnormality fall in the Normal category [3]. We have used an equal number of images in order to deal with the class imbalance problem. The dataset contains some images in which signals of different leads were merged. Such images are not included during the experimentation to ensure fair performance assessment. Table 2 shows the number of images per class during the experimentation process.

## 4.2 Experimental setup

We have used 5 classes present in the dataset for training our Shuffle SwishNet-181 architecture. All experiments are performed on a core i-5 processor, 4 GB RAM, and a 64-bit operating system. During experiments, MATLAB 2021 is used for the implementation of the method. The 'adam' optimizer, with maximum Epochs of 40 and a minimum batch size of 18 is used. The learning rate is set to 0.001 while no augmentation is applied during experimentations. Moreover, 80% of the dataset is used for training purposes and the rest 20% for testing. Preprocessing of the ECG data took around 0.2 s per ECG image. In total, the proposed approach required approximately 0.5 s per image which included feature extraction, and model prediction. This time complexity can be significantly reduced in GPU-supported machines.

#### 4.2.1 Evaluation parameters

The accuracy, sensitivity, specificity, F1-score, and AUCROC are used for the evaluation of the proposed model. Accuracy measures the number of correctly identified cases among

**Table 2** Number of images per class

Experiments	Number of images in each class
5- class	196
COVID-19 vs. Normal	250
COVID-19 vs. MI	234
COVID-19 vs. HB	246
COVID-19 vs. PMI	196
COVID-19 positive vs. COVID-19 negative	250

the total number of studied cases. Equation 3 is used to compute the accuracy of Shuffle SwishNet-181. Sensitivity explains what proportion of all positive cases is correctly identified as positive cases. Similarly, specificity explains what proportion of all negative cases is correctly identified as negative cases. F1-score is a harmonic mean of precision and recall, sensitivity is also known as recall while precision measures the proportion of positive cases that are positive. These measures are computed as follows:

$$Accuracy = \frac{TP + TN}{TP + FP + FN + TN}$$
(3)

$$Sensitivity = \frac{TP}{TP + FN} \tag{4}$$

$$Specificty = \frac{TN}{TN + FP} \tag{5}$$

$$F1 - Score = 2 \times \frac{Precision \times Recall}{Precision + Recall}$$
 (6)

#### 4.3 Performance evaluation

This section comprises the details of different experiments carried out to assess the performance of our method for reliable detection of COVID-19. Moreover, we have also provided a discussion on the results of these experiments.

#### 4.3.1 Assessment of proposed method for binary classification

To assess the capability of our proposed model for effective binary classification, a multistage experiment is designed to distinguish between COVID-19 patients and normal people, as well as between COVID-19 and other cardiovascular patients. More precisely, this experiment includes the classification between COVID-19 and Normal, COVID-19 and MI, COVID-19 and HB, and COVID-19 and PMI. The biasing effect is removed by using an equal number of images in each class. Details of the number of images used during experimentation are discussed in Table 2. The proposed model achieves an accuracy of 99% in the case of COVID-19 vs. Normal, 99.4% in the case of COVID-19 vs. MI, 98.8% in the case of COVID-19 vs. HB, and 98.7% in case of COVID-19 vs. PMI. The detailed class-wise results in terms of accuracy, sensitivity, specificity, and F1-score are provided in Table 3. These results illustrate the effectiveness of our model for reliable classification of

Table 3 Binary classification results

Experiment	Accuracy	Sensitivity	Specificity	F1-Score
COVID-19 vs Normal	99.0%	99.20%	98.88%	99.00%
COVID-19 vs MI	99.4%	98.72%	100%	99.35%
COVID-19 vs HB	98.8%	97.97%	99.59%	98.77%
COVID-19 vs PMI	98.7%	98.98%	98.47%	98.73%



COVID-19 vs each other respective class of images. Accuracy of 99% between COVID-19 ECG and Normal person ECG explains that there is a significant difference between Normal person ECG and COVID-19 ECG because patients during COVID-19 develop ECG abnormalities. The experiments performed between COVID-19 and other cardiovascular patients show that the features developed by COVID-19 are also different from MI, HB, and PMI patients. The accuracy between COVID-19 and HB is slightly lower because an abnormal heartbeat is one of the symptoms of COVID-19. These experiments show that COVID-19 patients develop ECG characteristics that are different from other classes. The results proved that Shuffle SwishNet-181 accurately detects COVID-19 patients from Normal, MI HB, and PMI patients.

The confusion matrix analysis is designed for each stage of this experiment to depict the misclassification rate (both false positives and false negatives) as shown in Fig. 3. Among 500 images, 5 images are incorrectly classified by the proposed model, which includes 3 images of COVID-19. In COVID-19 vs MI, all COVID-19 patients are correctly classified

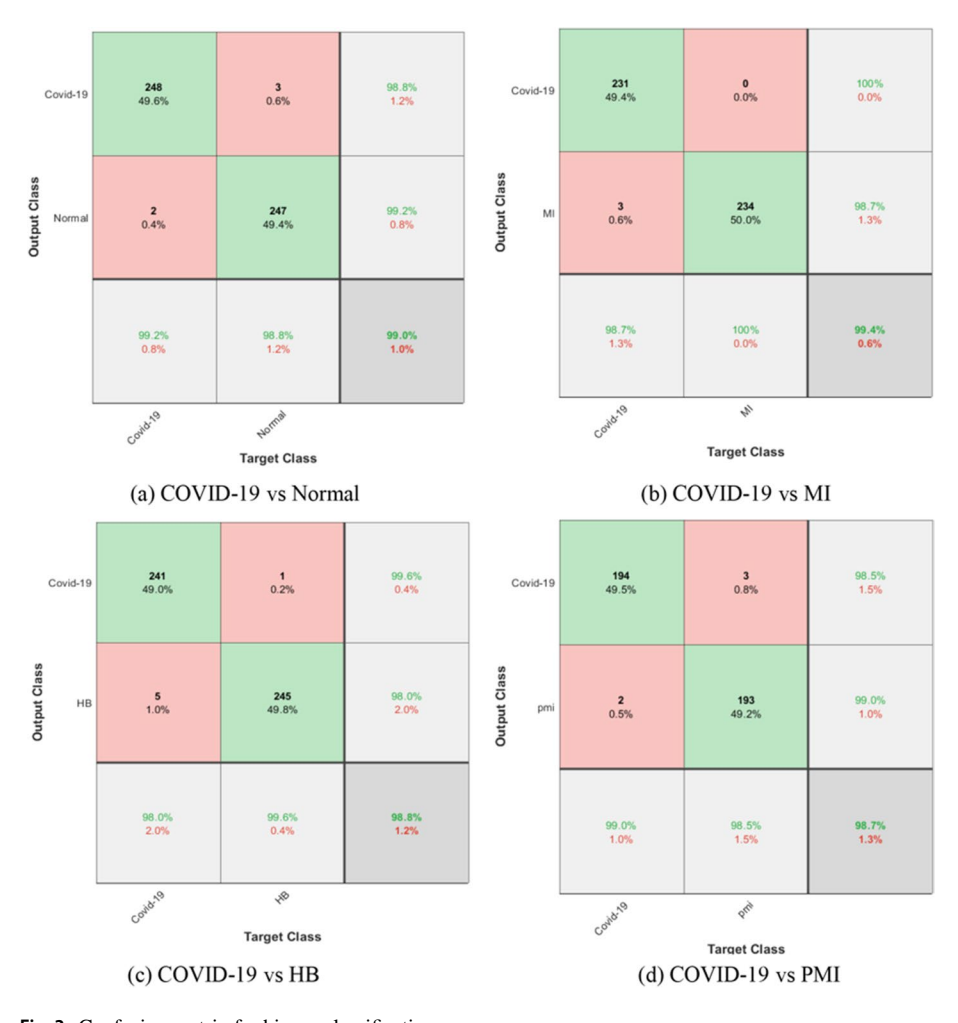


Fig. 3 Confusion matrix for binary classification

by the proposed model and only 3 MI images are identified as COVID-19 positive. In the case of COVID-19 vs PMI, 387 images are correctly identified out of 392 images. These results show that HB and COVID-19 ECG images have some similarities as 6 images are incorrectly classified out of 494 images. These results conclude that our proposed model has the capability to identify COVID-19 positive patients.

The AUC-ROC is also generated to portray the class-wise classification accuracy of our model. The proposed model achieved the AUC-ROC of 99.95% for COVID-19 vs Normal, 99.49% for COVID-19 vs HB, 99.84% for COVID-19 vs MI, and 99.73% for COVID-19 vs PMI. The AUC-ROC graphs are presented in Fig. 4, which shows the effectiveness of the Shuffle SwishNet-181 model for reliable classification of the COVID-19-affected people from the Normal, MI HB, and PMI patients.

## 4.3.2 Assessment of proposed method for multi-class classification

To assess the capability of our proposed model for effective multi-class classification, we designed an experiment to distinguish between the five classes i.e., COVID-19, MI, PMI, HB, and normal. For this experiment, all of the five classes present in the dataset are utilized. The macro F1-score is computed using a non-weighted average of the F1-score of

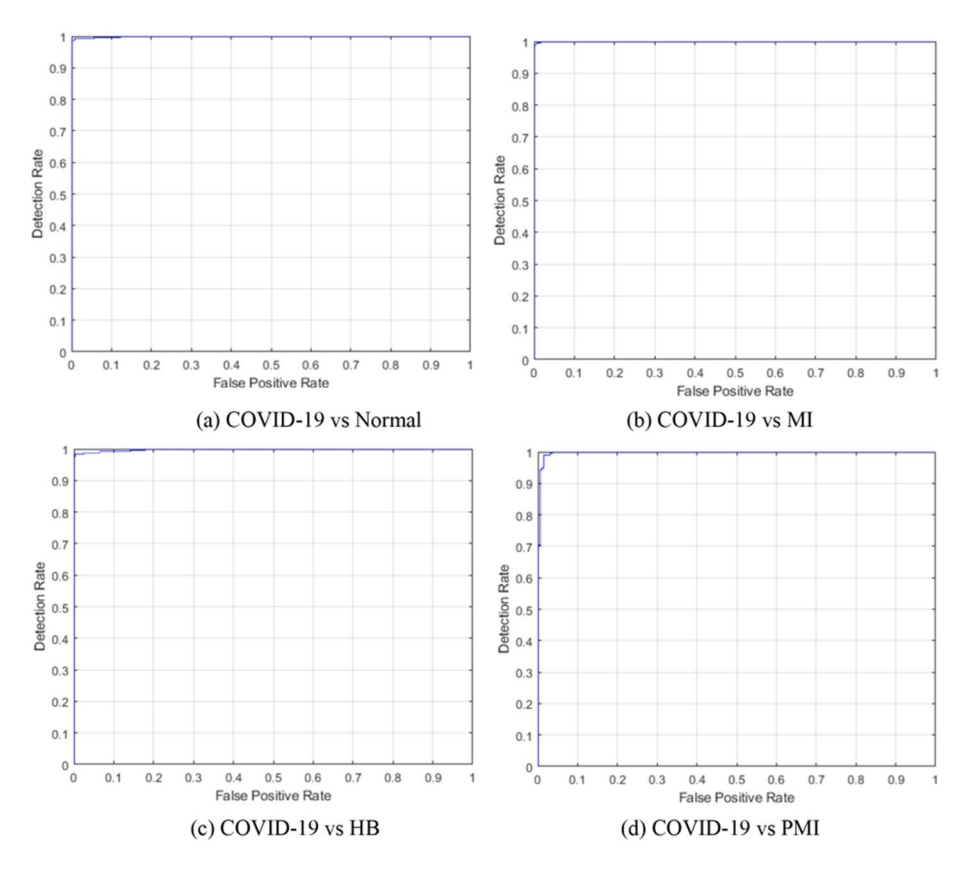


Fig. 4 AUCROC curves for binary classification

Content courtesy of Springer Nature, terms of use apply. Rights reserved.

**Table 4** Results of multiclass classification

Metric	Value
Accuracy	91.5%
Sensitivity	91.2%
Specificity	97.4%
F1-score	91.4%

**Fig. 5** Confusion matrix for 5-class classification

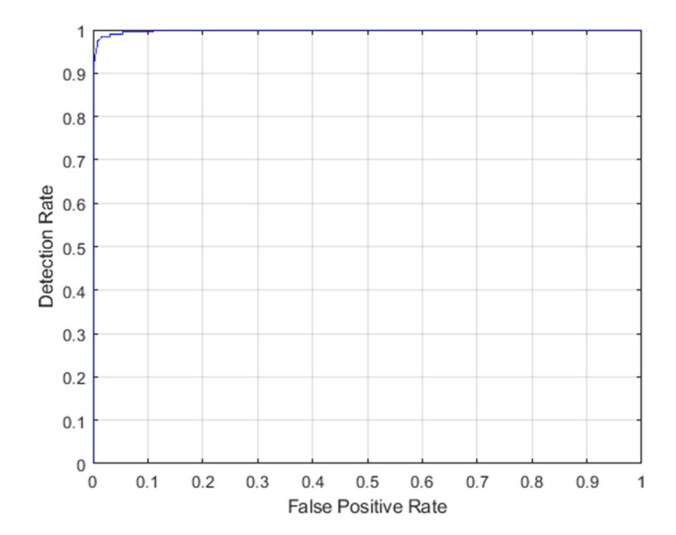


each class. Table 4 presents the details of the results of the proposed model on multiclass classification (Fig. 5).

AUC-ROC is calculated by comparing each class with other classes e.g., COVID-19 with Normal, COVID-19 with MI, COVID-19 with HB, and COVID-19 with PMI. After computing the AUCROC of all combinations we calculated the mean of all AUC values. Figure 6 shows that the proposed model covers 99.86% area under the curve for five class classification. It is noticeable that Shuffle SwishNet-181 can differentiate among COVID-19, Normal, MI, HB, and PMI patients effectively.

We also generated the Confusion matrix of multiclass classification. It is observable from Fig. 5 that the proposed model achieves 91.5% of accuracy. From Table 4, it is observable that the model achieved an F1-score of 91.4%, 97.4% specificity, and 91.2% sensitivity which is slightly lower than specificity. In the presence of different cardiovascular patients, 8.5% COVID-19 positive patients were incorrectly classified. Although, COVID-19 patients have different features still there exist similarities in the features among these classes. This similarity is the main reason for the drop in the sensitivity of Shuffle SwishNet-181 when it classifies all five classes simultaneously. It is noticeable from Fig. 5 that precision drops while classifying COVID-19 with HB and COVID-19 with PMI. This





shows that features of COVID-19-affected ECGs have more resemblance with HB and PMI classes. A specificity of 97.4% proves that Shuffle SwishNet-181 classifies non-COVID-19 patients effectively. The overall accuracy of 91.5% explains that Shuffle SwishNet-181 is effective even in the presence of other cardiovascular patients.

## 4.4 Comparison with existing methods

The main objective of this experiment is to assess the effectiveness of the proposed method over existing COVID-19 detection methods. For this purpose, the proposed model is compared with Mehmet et al. [20] and Attallah [5] as the study also used the same dataset for evaluation as adopted in the proposed work. Mehmet et al. focused mainly on binary classification whereas the method is evaluated on both the binary and multiclass classification. The author [20] extracted numerical features from ECG images and mapped the extracted features using hexaxial mapping. This conversion process has a risk that an error can be easily introduced in the classification data. An experiment is conducted in which we classify negative class (combined Normal, MI, and HB images as a negative class) and COVID-19. In COVID-19 and Normal classification, the hexaxial mapping model attained an accuracy of 96% while in COVID-19 and Negative (which included Normal, MI, and HB images) the model achieved 91% accuracy. Attallah focused on binary classification which includes COVID-19 and Normal classification and three-class classification which include COVID-19, cardiac disorders (which included HB, MI, and PMI), and Normal class. Results of the proposed model are slightly increased in the case of COVID-19 vs Normal class, however, in multiclass 3 separate classes for HB, MI, and PMI patients have been used while authors of the ECG BIO-Net model used all these 3 classes in a single class. Table 5 shows the comparison of our proposed model with Mehmet et al. and ECG Bio-net. Instead of converting ECG images into a matrix like Mehmet et al., the segmentation and opening process is used so that images remain the same during the whole preprocessing phase. The preprocessing performed on input images enhanced the feature extraction and inversing of limbs lead providing more angles to view heart electric activity. Ahmed et al. utilized three different CNN models for the classification of COVID-19 and Normal images. This study utilized imbalanced data for experiments. While the proposed

Experiment	Metric	ECG BIO-NET	Hexaxial map- ping method	[2]	Proposed model
COVID-19 vs. Normal	Accuracy	98.80%	96.20%	98.81%	99.00%
	Specificity	98.80%	94.00%		98.80%
	F1-Score	98.80%	96.30%	98.81%	99.00%
	AUC	_	99.15%		99.90%
COVID-19 vs. Negative	Accuracy	-	93.00%		98.40%
	Specificity	-	90.00%		99.60%
	F1-Score	-	93.20%		98.30%
	AUC	_	94.48%		99.40%

**Table 5** Comparison with existing methods

methodology also provides a comparison of COVID-19 patients with other cardiovascular diseases which shows that the model is not only effective against COVID-19 vs Normal classification but also effective in detecting COVID-19 against other heart-diseased patients.

## 4.5 Interpretability analysis of proposed Shuffle SwishNet-181 model

The interpretation of deep learning models is required to better explain their black-box nature. For this purpose, an experiment is designed to visualize the working of the proposed model by showing the top priority features extracted by the Shuffle SwishNet-181 model. Class activation mapping, gradient-based class activation mapping, and score-based class activation mapping are common when interpreting deep learning models in medical imaging-related tasks. Score-cam is based on class activation mapping but resolves the issues of noise involvement that were present in CAM and provides more explanation. Grad-Cam performs mapping based on a gradient which is considered unstable and produced noise in gradient-based maps. Score-cam does not depend on the gradient therefore change in gradient does not affect the performance of the Score-cam. This method works on the theme of perturbation-based training in which it creates a mask on various regions of an input image and calculates the change in the target class. CAM, grad-Cam, and score-Cam are used during trials and score-cam was found to provide the best visualization of the proposed model. The resized input image is passed to the Shuffle SwishNet-181 method for classification. The last convolution layer is mainly involved in extracting deep features and passes these features to global average pooling. The feature map coming from the last convolutional layer is normalized using the activation function and converted the feature map into a 3-channel map. In the last step, the dot product of the actual image and the feature map is performed. During the feature extraction and classification phase, Score-map shows the top priority feature coming from the last convolution layer of Shuffle SwishNet-181. For feature extraction, the deep red color represents the highest priority region, and the blue area represents the least priority region. It is noticeable in Fig. 7 where most of the signals located areas are deep red in color which represents a top priority feature. The visualization process revealed that the Shuffle SwishNet-181 effectively gives importance to those parts of the image where signals are located. This process makes the results of the proposed model more trustworthy and satisfactory.

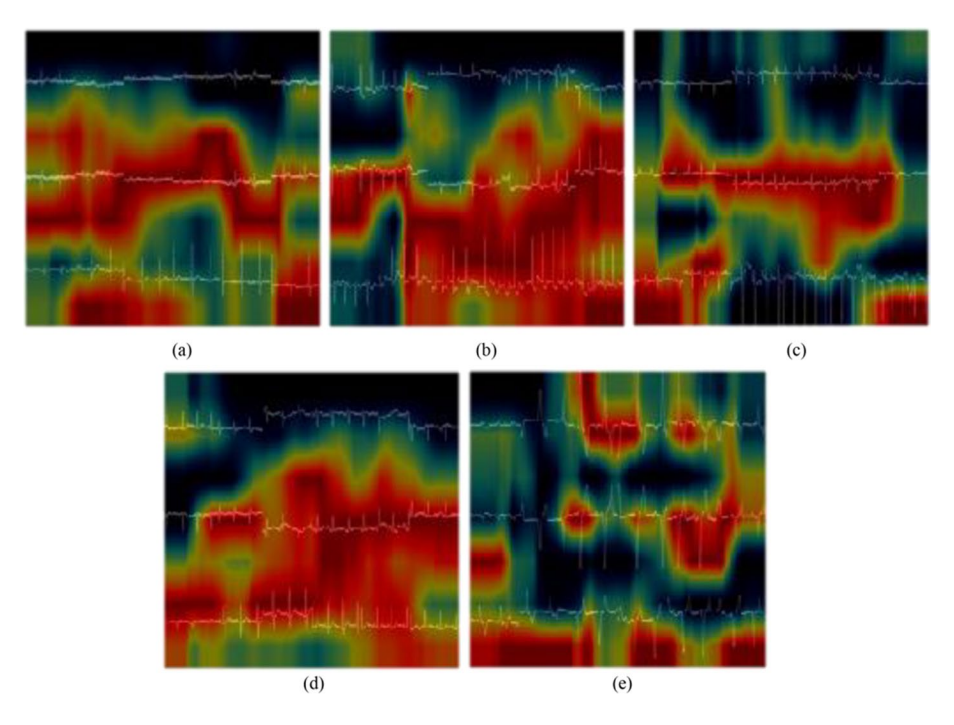


Fig. 7 Visualization of top priority features: (a) COVID-19 Image, (b) Normal Image, (c) MI, (d) HB, (e) PMI

#### 4.5.1 Statistical evaluation of shuffle swishNet-181

We designed an experiment to examine the statistical significance of the proposed Shuffle SwishNet-181 model against customized versions of the base ShuffleNet model. The main objective of this experiment was to analyze the impact of different components of the deep learning model such as activation functions, layer architecture, etc., on the outcome of COVID-19 classification. For this purpose, we compared the performance of our Shuffle SwishNet-181 model against the base and customized versions of ShuffleNet. More precisely, the architecture of base ShuffleNet model contains 172 layers and employs ReLU activation function, whereas, the customized ShuffleNet model used in this experiment includes 9 additional layers but keeps the same activation function (ReLU). On the other hand, our Shuffle SwishNet-181 model contains 181 layers and employs the Swish activation function to better address the issues of dying ReLU problem. The comparative results in terms of accuracy, F1-score, precision, and recall are provided in Table 6, which indicates that the Shuffle SwishNet-181 model outperformed all versions of ShuffleNet.

Shuffle SwishNet-181 architecture uniquely divides layers into different units, with the last nine layers forming the output unit. This allows for the output features to be passed to the classification layers, enhancing the model's classification performance. The superiority of Shuffle SwishNet-181 over basic ShuffleNet and customized ShuffleNet can be attributed to several factors. The Swish activation function used in Shuffle SwishNet-181 outperforms the ReLU activation function used in the basic ShuffleNet model. The swish function can help prevent

**Table 6** Comparative Evaluation of Shuffle SwishNet-181 with base and customized ShuffleNet models

Evaluation Metrics	ShuffleNet	Customized ShuffleNet	Shuffle Swish- Net-181
Accuracy	98.60%	97.20%	99.00%
F1-score	98.50%	97.71%	98.80%
Precision	99.00%	98.23%	99.00%
Recall	98.00%	95.00%	99.0%

numerical instability and diverging gradients that can occur with ReLU, leading to better training convergence and enhanced learning capacity in deep networks. The results in Table 6 indicate that the Shuffle SwishNet-181 model outperformed all other models in terms of accuracy, F1-score, precision, and recall, with statistically significant differences observed across all performance metrics. These findings provide compelling evidence of the effectiveness of our model and its ability to outperform the basic ShuffleNet and Customized ShuffleNet models for COVID-19 classification.

#### 5 Conclusion

This study has suggested an effective framework for reliable automated detection and diagnosis of COVID-19 patients through their ECG. Our proposed model can detect COVID-19 patients even in the presence of other cardiovascular patients. Results of the experiments proved that our model noticeably distinguishes COVID-19 patients from normal and other cardiovascular disease patients using ECG trace images. We also visualized the working of our model using a score-cam method to show the top priority features selected by our Shuffle SwishNet-181 for classification. We found that Shuffle SwishNet-181 precisely gives priority to areas of the image where signals are located. Our experiments have proved that ECG can be an effective source for the detection, diagnosis, and finding of the criticality of COVID-19. We conclude that the proposed model will assist current techniques of testing and improve the quality of testing and diagnosis. Research on COVID-19 and its relation to cardiovascular disease still needs more attention. Therefore, we plan to extend this work to find the correlation between COVID-19 and cardiovascular disease.

**Acknowledgements** The authors would like to thank the Multimedia Signal Processing (MSP) research lab at UET-Taxila for providing the lab resources to conduct this research.

Data availability The dataset used in the current study is available publicly.

(https://www.researchgate.net/publication/348594203\_ECG\_Images\_dataset\_of\_Cardiac\_and\_COVID-19\_Patients).

Data sharing not applicable to this article as no datasets were generated during the current study.

#### **Declarations**

Conflicts of interest The authors declare that they have no conflicts of interest.

## References

- Acharya UR, Fujita H, Oh SL, Hagiwara Y, Tan JHE, Adam M, Tan RS (2019) Deep convolutional neural network for the automated diagnosis of congestive heart failure using ECG signals. Appl Intell 49:16–27. https://doi.org/10.1007/s10489-018-1179-1
- Sakr AS, Pławiak P, Tadeusiewicz R, Pławiak J, Sakr M, Hammad M (2023) ECG-COVID: An end-toend deep model based on electrocardiogram for COVID-19 detection. Inf Sci 619:324–339. https://doi. org/10.1016/j.ins.2022.11.069
- Khan AH, Hussain M, Malik MK (2021) ECG Images dataset of Cardiac and COVID-19 Patients. Data Brief 34:106762. https://doi.org/10.1016/j.dib.2021.106762
- Mangal A, Kalia S, Rajgopal H, Rangarajan K, Namboodiri V, Banerjee S, Arora C (2020) CovidAID: COVID-19 Detection Using Chest X-Ray. arXiv preprint arXiv:2004.09803. [eess.IV]. https://doi.org/ 10.48550/arXiv.2004.09803
- Attallah O (2022) ECG-BiCoNet: An ECG-based pipeline for COVID-19 diagnosis using Bi-Layers of deep features integration. Comput Biol Med 142:105210. https://doi.org/10.1016/j.compbiomed.2022. 105210
- Pavri BB, Kloo J, Farzad D, Riley JM (2020) Behavior of the PR interval with increasing heart rate in patients with COVID-19. Heart Rhythm 17(9):1434–1438
- Chowdhury MR, Mas-ud MA, Ali MR, Fatamatuzzohora M, Shimu AS, Haq MA, Islam MA, Hossain, MF, Hosenuzzaman M, Islam MM, Hasan MF (2021) Harmful effects of COVID-19 on major human body organs: a review. J Pure Appl Microbiol 15(2):500–511. https://doi.org/10.22207/JPAM.15.2.14
- Arias-Garzón D, Alzate-Grisales JA, Orozco-Arias S, Arteaga-Arteaga HB, Bravo-Ortiz MA, Mora-Rubio A, Saborit-Torres JM, Serrano JÁM, de la Iglesia VM, Cardona-Morales O, Tabares-Soto R (2021) COVID-19 detection in X-ray images using convolutional neural networks. Mach Learn Appl 6:100138. https://doi.org/10.1016/j.mlwa.2021.100138
- Kaliyaperumal D, Bhargavi K, Ramaraju K, Nair KS, Ramalingam S, Alagesan M (2022) Electrocardiographic Changes in COVID-19 Patients: A Hospital-based Descriptive Study. Indian J Crit Care Med: Peer-Rev Off Publ Indian Soc Crit Care Med 26(1):43. https://doi.org/10.5005/jp-journals-10071-2404543-48
- Dey N, Roy S, Bhandari AK (2022) ECG-BiCoNet: An ECG-based pipeline for COVID-19 diagnosis using Bi-Layers of deep features integration. Comput Biol Med 130:105210
- 11. Crawford J, Doherty L (2012) Practical aspects of ECG recording. M&K publishing
- ECGwave.com (2022) ECG and Echo learning. https://ecgwaves.com/topic/ekg-ecg-leads-electrodessystems-limb-chest-precordial/. Accessed 23 Jan 2022
- Hussain E, Hasan M, Rahman MA, Lee I, Tamanna T, Parvez MZ (2021) CoroDet: A deep learning based classification for COVID-19 detection using chest X-ray images. Chaos Solitons Fractals 142:110495. https://doi.org/10.1016/j.chaos.2020.110495. (ISSN 0960-0779)
- Angelia F, Spanevelloa A, De Pontia R, Viscaa D, Marazzatoa J, Palmiottoa G, Fecia D, Reboldic G, Fabbrid LM, Verdecchiae P (2020) Electrocardiographic features of patients with COVID-19 pneumonia. Eur J Intern Med 78:101–106
- Hafer Nate (2021) What's the difference between a PCR and antigen COVID-19 test? A molecular biologist explains. The Conversation. 9 8. https://theconversation.com/whats-the-difference-between-apcr-and-antigen-covid-19-test-a-molecular-biologist-explains-170917. Accessed 15 May 2022
- Barman HA, Atici A, Alici G, Sit O, Tugrul S, Gungor B, Okuyan E, Sahin I (2021) The effect of the severity COVID-19 infection on electrocardiography. Am J Emerg Med 46:317–322. https://doi.org/ 10.1016/j.ajem.2020.10.005317-322
- Wong HYF, Lam HYS, Fong AHT, Leung ST, Chin TWY, Lo CSY, Lui MMS, YinLee JC, Chiu KW-H, Chung T, Lee EYP, Wan EYF (2020) Frequency and Distribution of Chest Radiographic Findings in COVID-19 Positive. Radiolody 296(2):E72–E78. https://doi.org/10.1148/radiol.2020201160
- Ece İ, Koçoğlu M, Kavurt AV, Bağrul D, Gül AEK, Koca S, Çetin İİ, Parlakay ANÖ, Aksoy S (2021)
   Assessment of Cardiac Arrhythmic Risk in Children With Covid-19 infection. Pediatric cardiology 42(2):264–268
- López-Cabrera JD, Orozco-Morales R, Portal-Diaz JA, Lovelle-Enríquez O, Pérez-Díaz M (2021) Current limitations to identify COVID-19 using artificial intelligence with chest X-ray imaging. Health Technol 11(2):411–424. https://doi.org/10.1007/s12553-021-00520-2411-424
- Ozdemir MA, Ozdemir GD, Guren O (2021) Classification of electrocardiograms by using hexaxial feature mapping and deep learning BMC Med Inform Decis Mak 21(1):1–20. https://doi.org/10.1186/ s12911-021-01521-x
- Rafie N, Kashou AH, Noseworthy PA (2021) ECG Interpretation: Clinical Relevance, Challenges, and Advances. Hearts 2(4):505–513. https://doi.org/10.3390/505-513



- 22. World Health Organization (2021) WHO. https://covid19.who.int/. Accessed Nov 2021
- Struyf T, Deeks JJ, Dinnes J, Takwoingi Y, Davenport C, Leeflang MMG, Spijker (2021) Signs and symptoms to determine if a patient presenting in primary care or hospital outpatient settings has COVID-19. Cochrane Database Syst Rev CD013665. https://doi.org/10.1002/14651858.CD013665. pub2
- Rahman T, Akinbi A, Chowdhury ME, Rashid TA, Şengür A, Khandakar A, Islam KR, Ismael AM (2022) COV-ECGNET: COVID-19 detection using ECG trace images with deep convolutional neural network. Health Inf Sci Syst 10(1):1. https://doi.org/10.1007/s13755-021-00169-1
- Wang L, Lin ZQ, Wong A (2020) COVID-Net: A Tailored Deep Convolutional Neural Network Design for Detection of COVID-19 Cases from Chest Radiography Images. Sci Rep 10(1):1–12
- Li Y, Liu T, Tse G, Wu M, Jiang J, Liu M, Tao L (2020) Electrocardiograhic characteristics in patients with coronavirus infection: A single-center observational study. Ann Noninvasive Electrocardiol 25(6):e12805
- Anwar T, Zakir S (2021) Effect of Image Augmentation on ECG Image Classification using Deep Learning. In 2021 International Conference on Artificial Intelligence (ICAI). IEEE (pp 182–186). https://doi.org/10.1109/ICAI52203.2021.9445258
- Zhang X, Zhou X, Lin M, Sun J (2018) Shufflenet: an extremely efficient convolutional neural network for mobile devices. In Proceedings of the IEEE Conference on Computer Vision and Pattern Recognition, pp 6848–6856. https://doi.org/10.1109/CVPR.2018.00716
- Zhao D, Yao F, Wang L, Zheng L, Gao Y, Ye J, Guo F, Zhao H, Gao R (2020) A Comparative Study on the Clinical Features of Coronavirus 2019 (COVID-19) Pneumonia With Other Pneumonias. Clin Infect Dis 71(15):756–761

**Publisher's Note** Springer Nature remains neutral with regard to jurisdictional claims in published maps and institutional affiliations.

Springer Nature or its licensor (e.g. a society or other partner) holds exclusive rights to this article under a publishing agreement with the author(s) or other rightsholder(s); author self-archiving of the accepted manuscript version of this article is solely governed by the terms of such publishing agreement and applicable law.

#### **Authors and Affiliations**

# Tanees Riaz¹ · Ali Javed¹ · Majed Alhazmi² · Ali Tahir² · Rehan Ashraf³ ©

- Department of Software Engineering, University of Engineering and Technology, Taxila 47050, Pakistan
- College of Computer Science and Information Technology, Jazan University, 45142 Jazan, Saudi Arabia
- Department of Computer Science, National Textile University, Faisalabad, Pakistan

## Terms and Conditions

Springer Nature journal content, brought to you courtesy of Springer Nature Customer Service Center GmbH ("Springer Nature").

Springer Nature supports a reasonable amount of sharing of research papers by authors, subscribers and authorised users ("Users"), for small-scale personal, non-commercial use provided that all copyright, trade and service marks and other proprietary notices are maintained. By accessing, sharing, receiving or otherwise using the Springer Nature journal content you agree to these terms of use ("Terms"). For these purposes, Springer Nature considers academic use (by researchers and students) to be non-commercial.

These Terms are supplementary and will apply in addition to any applicable website terms and conditions, a relevant site licence or a personal subscription. These Terms will prevail over any conflict or ambiguity with regards to the relevant terms, a site licence or a personal subscription (to the extent of the conflict or ambiguity only). For Creative Commons-licensed articles, the terms of the Creative Commons license used will apply.

We collect and use personal data to provide access to the Springer Nature journal content. We may also use these personal data internally within ResearchGate and Springer Nature and as agreed share it, in an anonymised way, for purposes of tracking, analysis and reporting. We will not otherwise disclose your personal data outside the ResearchGate or the Springer Nature group of companies unless we have your permission as detailed in the Privacy Policy.

While Users may use the Springer Nature journal content for small scale, personal non-commercial use, it is important to note that Users may not:

- 1. use such content for the purpose of providing other users with access on a regular or large scale basis or as a means to circumvent access control;
- 2. use such content where to do so would be considered a criminal or statutory offence in any jurisdiction, or gives rise to civil liability, or is otherwise unlawful;
- 3. falsely or misleadingly imply or suggest endorsement, approval, sponsorship, or association unless explicitly agreed to by Springer Nature in writing;
- 4. use bots or other automated methods to access the content or redirect messages
- 5. override any security feature or exclusionary protocol; or
- 6. share the content in order to create substitute for Springer Nature products or services or a systematic database of Springer Nature journal content.

In line with the restriction against commercial use, Springer Nature does not permit the creation of a product or service that creates revenue, royalties, rent or income from our content or its inclusion as part of a paid for service or for other commercial gain. Springer Nature journal content cannot be used for inter-library loans and librarians may not upload Springer Nature journal content on a large scale into their, or any other, institutional repository.

These terms of use are reviewed regularly and may be amended at any time. Springer Nature is not obligated to publish any information or content on this website and may remove it or features or functionality at our sole discretion, at any time with or without notice. Springer Nature may revoke this licence to you at any time and remove access to any copies of the Springer Nature journal content which have been saved.

To the fullest extent permitted by law, Springer Nature makes no warranties, representations or guarantees to Users, either express or implied with respect to the Springer nature journal content and all parties disclaim and waive any implied warranties or warranties imposed by law, including merchantability or fitness for any particular purpose.

Please note that these rights do not automatically extend to content, data or other material published by Springer Nature that may be licensed from third parties.

If you would like to use or distribute our Springer Nature journal content to a wider audience or on a regular basis or in any other manner not expressly permitted by these Terms, please contact Springer Nature at